Thermochemical Nonequilibrium Modeling for Hypersonic Flows Containing Oxygen

Kevin Neitzel[*], Daniil Andrienko[†], and Iain D Boyd[‡]

University of Michigan, Ann Arbor, Michigan, 48109, USA

The simulation results for a set of thermochemical nonequilibrium models with a range of fidelity is compared to experimental data for shock tube and double-cone flows. The present work focuses solely on oxygen flows. The two-temperature (2T) model is the widely used approach for hypersonic analysis and is presented as the computationally efficient, lower fidelity modeling approach in this work. In contrast, the full state-to-state (STS), master equation approach is presented as the higher fidelity modeling approach. Both approaches have several available methods for obtaining rate data that are investigated. The STS method introduces a large master equation system that has been prohibitive due to its computational expensive for design applications. The present paper aims to understand the deficiencies of the standard 2T model when compared to detailed STS analysis. Additionally, the STS rates allow for detailed investigation of the effects that nonequilibrium and non-Boltzmann behavior have on the macroscopic behavior. This present work suggests a modified 2T model, the 2T-NENB (nonequilibrium, non-Boltzmann) model, that aims to capture STS model behavior in a computationally inexpensive, 2T model form. The performance of this modified model is compared with standard 2T model results, full STS model results, and experimental data. Additionally, areas of future improvement and computational expense are discussed.

Nomenclature

A, B	Millikan-White coefficients
E_v	Vibrational energy [J]
E_v^*	Equilibrium vibrational energy [J]
K_d	Total dissociation rate [cm^3/sec]
$k_{d,i}$	Dissociation rate from ith vibrational state [cm^3/sec]
$k_{v,v'}$	Transition rate from vibrational state v to v' [cm^3/sec]
μ	Reduced mass [kg]
P	Pressure [atm]
ρ	Density [kg/m^3]
T_t	Translational temperature [K]
T_v	Vibrational temperature [K]
τ_v	Vibrational relaxation time [sec]
v	Vibrational quantum state

I. Introduction

Computer simulation plays a primary role in analysis and design of hypersonic vehicle systems. This approach is taken due to the difficulties of reproducing high enthalpy flight conditions in ground test facilities. Past missions, including Mars Science Laboratory[1] , Stardust[2] , and Orion[3] , have relied heavily on CFD

---

[*]PhD Candidate, Department Aerospace Engineering, 1320 Beal Avenue, and Member of AIAA.
[†]Post-doctoral Research Fellow, Department Aerospace Engineering, 1320 Beal Avenue, and Member of AIAA.
[‡]Professor, Department of Aerospace Engineering, 1320 Beal Avenue, and AIAA Fellow.

American Institute of Aeronautics and Astronautics

modeling for analysis of the hypersonic phases of their missions. Thus, it is important to establish the capability of CFD simulation to accurately predict the flow field and surface properties for hypersonic flow conditions. Many hypersonic tunnel experiments have been performed at CUBRC,[5,6] specifically utilizing the CUBRC LENS-XX expansion tunnel. Previous comparisons between CFD and experimental data generated under hypersonic conditions at CUBRC have been performed for various flow compositions.[4] Comparisons for nitrogen flows have shown good agreement overall.[5] However, flows containing oxygen (both oxygen only and air-like compositions) have not shown good overall agreement.[5,6] It is suspected that nonequilibrium behavior of oxygen is a potentially significant contributer to the discrepancy in the results. Recent post-normal shock results,[7] including the results in this paper, compare with shock tube experimental data from Ibraguimova[30] and show that state-to-state modeling describes nonequilibrium behavior more accurately than the standard two-temperature modeling approach for hypersonic oxygen flows.

The two-temperature model is the widely used approach for hypersonic vehicle analysis.[14] For vibrational relaxation, the approach relies on a relaxation time equation that is a function of temperature to evolve the Landau-Teller equation for vibrational energy. The Millikan-White (MW) vibrational relaxation parameter formula is generally used, and correlates well with experimental data for many interactions.[15] However, the O_2-O system has a many body potential with a significant attractive component that is not consistent with the Landau-Teller theory. The MW predicted vibrational relaxation of the O_2-O system does not correlate well with experimental data.[5,16] The O_2-O system violates many of the assumptions that are present in the underlying Landau-Teller theory that dictates the temperature dependence of the Millikan-White formula. Park and others have adjusted the Millikan-White coefficients for O_2-O to correlate better with experimental data.[17] However, the previous work has assumed the temperature dependence dictated by the Landau-Teller theory. The vibrational relaxation of O_2-O is studied in this work using recently developed rates from a detailed quasi-classical trajectory (QCT) analysis.[18] Chemistry is captured by reaction rates that use Arrhenius-type rate coefficients. Additionally, the Arrhenius form uses the geometrically averaged temperature of the translational and vibrational temperature ($T_a = \sqrt{T_t T_v}$) in order to capture nonequilibrium, thermochemical coupling.

The state-to-state (STS) model is a higher fidelity approach to describing the vibrational energy mode. The STS model is much more computationally expensive since the population of each vibrational state is accounted for. The populations are evolved directly based on STS transition rates and dissociation rates. This approach allows for multi-quantum transitions and non-Boltzmann distributions to be captured.[19,20] There are two widely used methods for deriving the required STS transition rates. They are the forced harmonic oscillator (FHO) model of Adamovich[21–23] and the (QCT) analysis.[18,27] The FHO model is a semi-classical analytical method based on assumptions about the collision event and the form of the potential energy surface (PES). The analytical form of the FHO method makes it very attractive due to the low computational expense required to generate transition rates. The QCT method is more general and can be performed on any PES. The QCT method simulates thousands of individual collision events to calculate transition probabilities and rates for STS transitions and dissociation transitions. The QCT method is computationally expensive, but the recent increase in computational power has made it tractable for some systems. As mentioned, the results of a QCT analysis for O_2-O are investigated. In particular, the QCT transition rates will be reduced to a vibrational relaxation time, as well as used in a full STS analysis. The O_2-O_2 system has not been analyzed using the QCT method to date. The STS rates for O_2-O_2 utilize the FHO model.

STS rates allow for detailed information about the vibrational-translational energy transfer and dissociation. Specifically, an evaluation can be made for arbitrary combinations of translational temperature and vibrational temperatures or population distributions. This detail understanding from high fidelity STS rates allows for a reduced order model to be developed. It is desired to retain the framework of the 2T model due to its widespread use. The presented work will develop a modified version of the 2T model named the 2T-NENB (nonequilibrium, non-Boltzmann) model. The goal is to have a 2T-type model that is able to provide results that closely mimic the full STS analysis. This is extremely advantageous for hypersonic design work that can not currently handle the computational expense of full STS analysis.

In addition to shock tube flow comparisons, experimental data from CUBRC will be used for a double-cone configuration comparisons. This experimental data set only contains surface data so it will be a good evaluation of a hypersonic vehicle design scenario.

In summary, the presented work will focus on nonequilibrium modeling by comparing simulation results with experimental data for hypersonic oxygen flows. First, the effect of nonequilibrium modeling fidelity

American Institute of Aeronautics and Astronautics

is presented by comparing against the Ibraguimova experimental data for post-normal shock relaxation. This will provide the evaluation of the 2T models against high fidelity STS results and experimental data. Next, the effect of nonequilibrium modeling fidelity is presented using the CUBRC double-cone configuration experimental data. Finally, suggestions will be made for the most effective nonequilibrium modeling practices for oxygen flows as well as areas of future research for nonequilibrium CFD of hypersonic oxygen flows.

II. Thermochemical Nonequilibrium Modeling

The following subsections describe the various modeling methodologies for capturing thermochemical nonequilibrium behavior. Special emphasis will be placed on the differences in the models regarding the treatment of the vibrational nonequilibrium effect on vibrational-translational energy transfer and dissociation, in addition to the assumptions of the vibrational population distribution. These aspects are particularly important for the relaxation behavior of oxygen flows.

A. Two-Temperature Model (2T)

In the two-temperature (2T) model, nonequilibrium in the energy modes is captured by separating the translation energy, $E_t(T_t)$, and the vibrational energy, $E_v(T_v)$. The other energy modes are modeled, however they are assumed to be in equilibrium with either the translational or vibrational mode. The present work assumes that the rotational energy mode is in equilibrium with the translational mode and the electronic energy mode is in equilibrium with the vibrational mode. It should also be noted that the present work accounts for only the ground electronic states. Molecular oxygen is known to have accessible, low-lying electronic excited states, however that topic will be the focus of future investigations.

The vibrational energy evolution is governed by the Landau-Teller equation, Eq. (1).

$$\frac{d\,E_v}{d\,t} = \frac{E_v^* - E_v}{\tau_v} \tag{1}$$

The relaxation time, τ_v, in Eq. (1) can be obtained by various methods. The most widely used method is the Millikan-White relaxation time shown in Eq. (2). The values for A and B are unique for each species-pair interaction, and can be calculated based on the reduced mass and vibrational characteristic temperature, A=$0.00116\mu^{\frac{1}{2}}\theta^{\frac{4}{3}}$ and B = $0.015\mu^{\frac{1}{4}}$.

$$p\tau_v = exp(A\,(T^{-\frac{1}{3}} - B) - 18.42) \qquad [atm - sec] \tag{2}$$

The Millikan-White relaxation time is modified with the collision-limited correction term shown in Eq. (3) and Eq. (4). It is also referred to as the high temperature correction (HTC). The correction terms include the number density, n, and the mean particle velocity, c. In this work, σ_v^* is set to 3.0×10^{-21} m^2 as proposed by Park.[17]

$$\tau_{Park} = \frac{1}{n\,\sigma_v\,c} \qquad [sec] \tag{3}$$

$$\sigma_v = \sigma_v^* \left(\frac{50,000}{T}\right)^2 \qquad [m^2] \tag{4}$$

The Millikan-White relaxation time equation is derived from Landau-Teller theory. The Landau-Teller theory derives a particular temperature dependence for the relaxation time equation. The Millikan-White relaxation time retains the dominant temperature dependence of the Landau-Teller theory, and is known to describe many species interactions accurately, including the O_2-O_2 system. The present work adopts the Millikan-White relaxation time for the O_2-O_2 system.[17,25] However, the assumptions do not apply well to a system containing a molecule and an open shell atom, like the O_2-O system.[16,24,26] These types of systems deviate due to the effect of additional mechanisms such as non-adiabatic transitions and the possibility of atom exchange. The experimental data for the O_2-O system has been shown to not follow the Millikan-White suggested behavior. Park[17] proposed new Millikan-White coefficients for O_2-O, however, the same temperature dependence was still assumed to be consistent with Landau-Teller theory. O_2-O_2 has Millikan White coefficients of A=135.91 and B=0.030. The widely accepted Millikan White coefficients for O_2-O are A=47.7 and B=0.059.

American Institute of Aeronautics and Astronautics

In the 2T model, the dissociation process is treated by Arrhenius-type rate coefficients with the geometrically averaged temperature of the translational and vibrational temperature ($T_a = \sqrt{T_t T_v}$). The inclusion of the vibrational temperature implicitly defines the effect that vibrational nonequilibrium has on the dissociation behavior. The Arrhenius form is shown in Eq. 5. Additionally, the Arrhenius coefficients are summarized in Table 1. When a molecule dissociates, its vibrational energy is lost, and this effect must be accounted for in the model. Since the dissociating molecule could be at a low vibrational state or a high vibrational state, an assumption must be made as to an average energy loss due to dissociation. The present work assumes this vibrational energy loss due to dissociation to be 0.45 of the dissociation energy.

$$k_d = C \, T_a^n \, exp\left(-\frac{\theta_d}{T_a}\right) \qquad \left[\frac{cm^3}{s}\right] \tag{5}$$

	C	n	θ_d
O_2-O_2 (Park)	2.00×10^{21}	-1.5	59360
O_2-O (Park)	1.00×10^{22}	-1.5	59360

Table 1. Arrhenius parameters of dissociation reaction, pre-exponential factor is in cm^3/s/mole

One would expect that the vibrational-translational energy transfer and the dissociation would depend on the vibrational population distribution. It should be noted that the 2T methodology assumes that the vibrational population distribution is a Boltzmann distribution. This assumption is embedded in the formulation of the Landau-Teller equation and the dissociation method.

B. State-To-State Model (STS)

A detailed QCT analysis was performed by Andrienko and Boyd[18] for the O_2-O system. The final results are provided in a curve fit form as shown in Eq. 6 and Eq. 7. The transition rates for the O_2-O_2 system are taken from FHO analysis.[21–23, 25] These rates are used in a master equation approach as outlined in Ref. 8. It can be noted that a STS model explicitly represents the populations of each vibrational state. The evolution of the population distribution is driven by the STS rates and dissociation rates. There is no assumption made for the population distribution or the coupling between the vibrational relaxation and dissociation.

$$K_{v \to v'} = 1 \times 10^{-12} \exp[A + \frac{B}{\log(x)} + C\log(x)] \quad x = \frac{T}{1000} \qquad [\frac{cm^3}{s}] \tag{6}$$

$$\log(K_{v \to diss}) = A + B\log(T) - \frac{C}{T} \qquad [\frac{cm^3}{s}] \tag{7}$$

C. Modified Two-Temperature Model (2T-NENB)

A modified two-temperature model is presented that attempts to address some of the short comings of the standard two-temperature model. Previous work has shown that hypersonic oxygen flows can often contain vibrational nonequilibrium behavior and non-Boltzmann vibrational population distributions.[7, 19, 31] Both of these features have a strong effect on the flow field solution and cannot be captured with the standard 2T model.

In order for a thermochemical model to accurately represent hypersonic flows with oxygen, it needs to account for vibrational nonequilibrium and non-Boltzmann vibrational population distribution effects. The 2T-NENB (NonEquilibrium, Non-Boltzmann) model was developed by investigating the state-to-state transition and dissociation rates. Specifically, the state resolved rates can be used to understand the influence that vibrational nonequilibrium and non-Boltzmann distributions have on the macroscopic level vibrational-translational energy transfer and the total dissociation rate. Formally, a complete master equation analysis is required to capture the exact behavior of the effects in question. However, the present work is strictly concerned with flows that are dominated by post shock relaxation behavior. This focus allows for a number of assumptions to be made and a useful model to be developed.

One of the main areas of focus for this work is to apply the QCT calculated transition rates for O_2-O from Andrienko and Boyd.[18] A set of state-to-state transition rates was constructed using an accurate many-body

American Institute of Aeronautics and Astronautics

PES. The Varandas and Pais PES[18] generates 47 vibrational states and a maximum of 236 rotational levels for electronic ground-state molecular oxygen. Equation (8) presents the curve fit form of the vibrational relaxation parameter obtained from the QCT results.[18]

$$P\tau_{vib} = (ax^3 + bx^2 + cx + d) \times 10^{-8} \qquad [atm-sec] \tag{8}$$

Figure 1 compares the vibrational relaxation parameter from different methods for O_2-O (O_2-O_2 is also shown for reference). The experimental data for O_2-O is only available at relatively low temperatures (less than 4000K), which makes it difficult to infer the correct temperature dependence. Park and others have assumed the same form as the Landau-Teller temperature dependence. No temperature dependence is assumed in the QCT method. The QCT results deviate from the Landau-Teller temperature dependence. This is plausible, if not expected, given that the O_2-O system does not adhere to the assumptions of Landau-Teller theory.
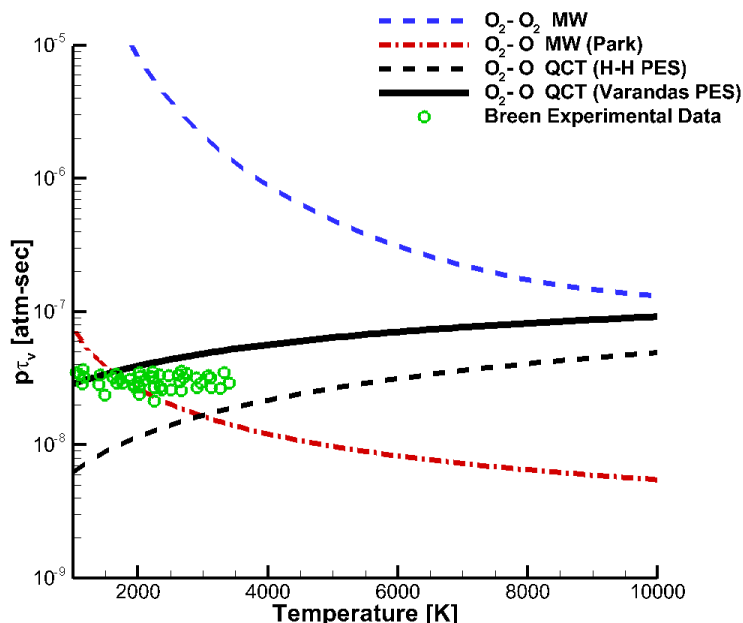
Figure 1. Vibrational relaxation parameter obtained from various models

The equilibrium dissociation rate for O_2-O has also been extracted from the QCT data. It is shown in Table 2.

	C	n	θ_d
Varandas PES	1.725×10^{18}	-0.4037	60540.0

Table 2. Arrhenius parameters of dissociation reaction, pre-exponential factor is in $cm^3/s/mole$

The utilization of the state resolved rates is potentially very powerful. It allows any vibrational distribution to be evaluated for vibrational-translational energy transfer and total dissociation rate. The 2T-NENB model takes the form of the standard 2T model but has modification terms to account for nonequilibrium and non-Boltzmann effects. The dissociation behavior has a dominating influence on the overall solution. The development of these dissociation modifications are shown in detail below.

The dissociation portion of the 2T model uses Arrhenius-type rate coefficients. Generally, the nonequilibrium effect on the dissociation rate is captured by the use of a control temperature in the dissociation rate equation. The most popular control temperature formulation is by Park ($T_a = \sqrt{T_t T_v}$). Other control temperature formulations have been suggested.[29] With accurate state-to-state rates from QCT for the O_2-O

system and rates from FHO for the O_2-O_2 system, the best formulation can be selected. A range of translational and vibrational temperature combinations were used to determine the accurate total dissociation rate. The focus of this specific exercise is to study the nonequilibrium effect on total dissociation rate. All populations for this exercise are assumed to have a Boltzmann distribution. The effects of non-Boltzmann distribution will be investigated later in this section.

Figure 2 shows the QCT generated total dissociation rate for a number of translational temperature and vibrational temperature combinations for the O_2-O system. The equilibrium total dissociation rate is also plotted. The figure suggests that a non-symmetrical treatment of the control temperature is needed to capture both heating and cooling behaviors properly.
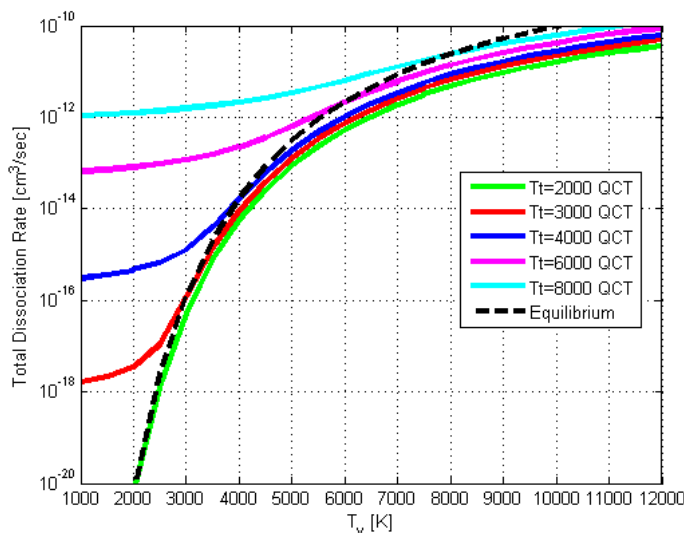
Figure 2. O_2-O Total Dissociation Rate for Combinations of Translational and Vibrational Temperatures (Boltzmann)

Additionally, figure 3 compares the nonequilibrium effect predicted dissociation rates by the Park model against the QCT based dissociation rates. The Park model captures the behavior near equilibrium for heating flow conditions. However, the Park model deviates from the QCT based dissociation rates for strong nonequilibrium conditions and cooling flows.

The presented work aims to develop a reduced order model based on the understanding of the detailed QCT results. As previously mentioned, the developed model should fit within the 2T framework since it has widespread use. The most efficient way to implement the nonequilibrium effect on dissociation rate is to make a correction to the control temperature. The equation below presents the form of the control temperature that was selected.

$$T_a = T_t \left(A + (1 - A) \left(\frac{T_v}{T_t} \right)^B \right) \tag{9}$$

Figure 4 presents the final selection of the control temperature parameters. Specifically, during heating, A=0.65 and B=3.0 and during cooling, A=0.2 and B=1.0 for the O_2-O system. The same procedure was applied to the O_2-O_2 system resulting in A=0.65 and B=3.0, and A=0.1 and B=1.0 for heating and cooling, respectively. The presented model is able to capture the nonequilibrium effect on dissociation rate over a larger range than the Park form of the control temperature.

Next, the state resolved QCT rates are used to determine the effect of a non-Boltzmann vibrational distribution on the total dissociation rate. In principle, the vibrational distribution can be anything. However, in relevant hypersonic flow conditions, the distributions deviate from Boltzmann in very specific ways. The presented work will focus on post shock relaxation conditions to guide the study of non-Boltzmann distributions. Figures 5 and 6 show the typical evolution of the vibrational distribution after a shock. The distribution quickly becomes overpopulated relative to the Boltzmann distribution after the shock. As the
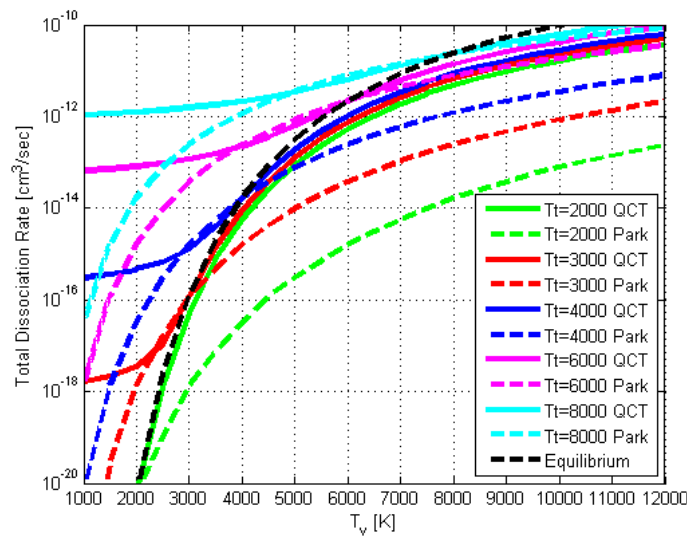
American Institute of Aeronautics and Astronautics

Figure 3. O$_2$-O Total Dissociation Rate from QCT Analysis and Park Nonequilibrium Model
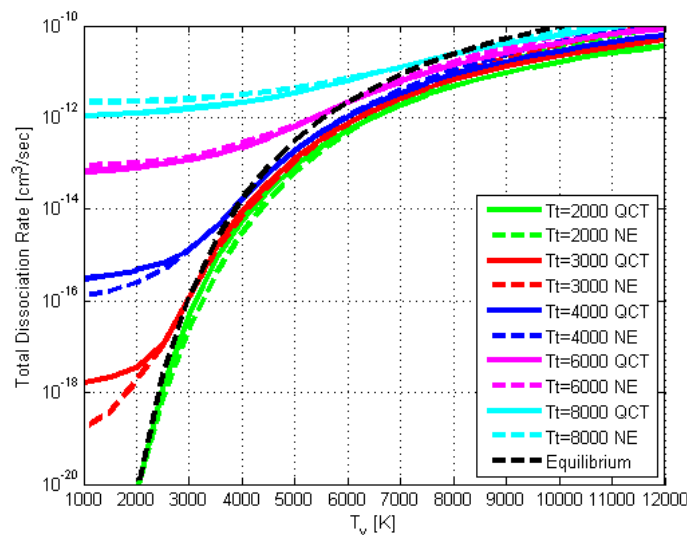

Figure 4. O$_2$-O Total Dissociation Rate from QCT Analysis and Presented Nonequilibrium Model

distribution evolves, the distribution becomes a Boltzmann for an instance before continuing to an underpopulated tail distribution. This underpopulated tail distribution corresponds to a QSS or near QSS behavior region. This evolutionary behavior of the population has been observed in other studies[7, 19] and with other species.[31]

Now that the type and range of non-Boltzmann distributions have been identified, a model form must be selected. In general, the distribution at a given time or space depends on the evolutionary history of that particular set of molecules. The modifications proposed in this study aim to fit into the framework of the standard 2T model. With this restriction, the only information about the vibrational population history is in the form of the vibrational temperature. That means that an assumption about the population history must be made in order to be useful in this framework. This could be considered the largest concession in generality for this model. However, the loss in generality leads to more convenience and a much reduced computational expense. Using the QCT rate results and post shock relaxation information as a guide, a
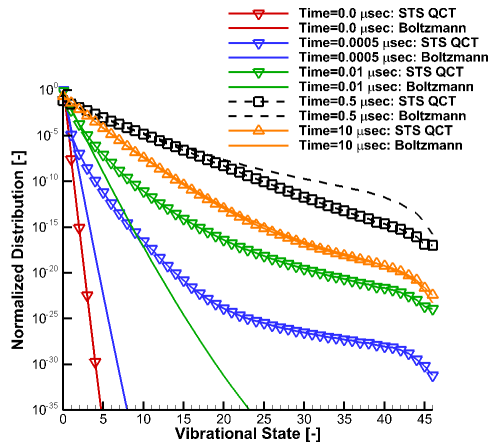
American Institute of Aeronautics and Astronautics

Figure 5. Vibrational population distribution evolution, sample
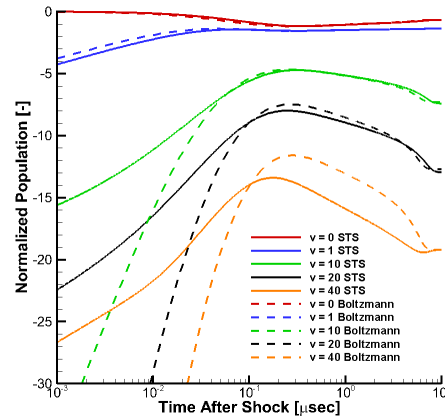

Figure 6. Vibrational state population evolution, sample

scale factor has been placed on the total dissociation rate to account for non-Boltzmann distribution effects. Specifically, the scale factor of the form $(T_{v_{crit}}/T_v)^C$ was selected. This represents a temperature ratio raised to a power, where $T_{v_{crit}}$ is the critical vibrational temperature where the distribution switches from overpopulated to under populated and C is a constant parameter that controls the effect away from this critical temperature. Notionally, this scale parameter will act to increase the total dissociation rate for an overpopulated distribution and decrease it for an underpopulated tail distribution.

Figures 7 and 8 present the effect of both an overpopulated and underpopulated distribution. These results are used in the selection of the nonequilibrium model parameters.
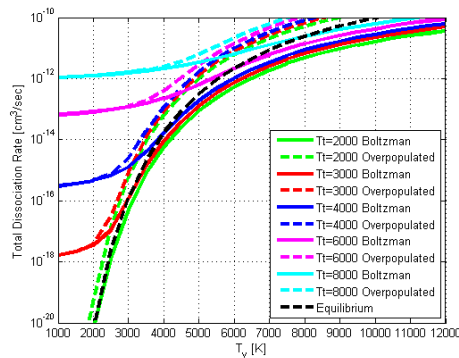
Figure 7. Total Dissociation Rate from QCT Analysis for an Overpopulated Boltzmann Distribution
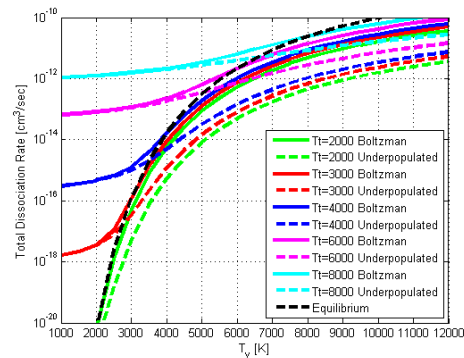

Figure 8. Total Dissociation Rate from QCT Analysis for an Underpopulated Boltzmann Distribution

The study selected $T_{v_{crit}}$=3500K and C=3.0 for both O_2-O and O_2-O_2 systems. The $T_{v_{crit}}$ parameter appears to be similar or be universal in some sense. These parameter values are selected with the assumption of using it for a post shock, heating type flow. Application to a cooling flow is not investigated in the presented work. The final form of the total dissociation rate is in the following form.

$$K_{diss} = \left(\frac{T_{crit}}{T_v}\right)^C K_{diss,eq}(T_a) \tag{10}$$

D. Flow Solvers

The nonequilibrium modeling techniques in this work are applied to two different flow scenarios: 1D shock tube flow and 2D double cone flow. Each flow scenario utilizes a unique flow solver and both will be described in this section.

American Institute of Aeronautics and Astronautics

1. 1D Shock Tube Flow Solver

In the present work, the post normal shock calculations use the jump conditions derived from the Rankine–Hugoniot relations. The derivation assumes that the electronic and vibrational modes are frozen across the shock wave. The flow downstream of the shock wave is calculated by solving the one-dimensional compressible flow equations combined with the conservation equations associated with the vibrational energy mode. The compressible flow equations are shown in equation 11.

$$\frac{\partial}{\partial x} \begin{pmatrix} \rho_s\, u \\ \rho\, u^2 + p \\ \rho\, u\left(h + u^2/2\right) \end{pmatrix} = \begin{pmatrix} \omega_s \\ 0 \\ 0 \end{pmatrix}, \tag{11}$$

The variables ρ and ρ_s are the densities of the mean flow and of the species s, u, P, h are the mean flow velocity, pressure and enthalpy, ω_s is the production rate of species s due to chemical reactions. The system of Euler equations 11 is closed by the ideal gas law. The conservation equations for vibrational energy are formulated individually for the 2T and STS models and given in the following sections.

In the two-temperature (2T) model, nonequilibrium in the energy transfer is described by separating the trans-rotational energy, $e_t(T)$, and the vibration-electronic energy, $e_v(T_v)$. The present work accounts for only the ground electronic state. The conservation equation for vibrational energy has the following appearance:

$$\frac{\partial\left(\rho e_v\right)}{\partial x} = \rho_{O_2}\frac{e_v^\star - e_v}{\tau_v} + \dot{\omega}_{O_2} C_{VD} D_e, \tag{12}$$

where $\dot{\omega}_{O_2} = R\left(T_a\right)n_O^3 - D\left(T_a\right)n_{O_2}n_O$, D and R are the global dissociation and recombination rate coefficients evaluated at some effective temperature T_a defined below, n is the number density, e_v and $e_v^\star$ are the mean vibrational energies evaluated at translational (T) and vibrational (T_{vib}) temperatures, respectively, C_{VD} is the vibration-dissociation coupling coefficient that indicates the average loss of vibrational energy in collision of particles that leads to dissociation, τ_v is the relaxation time of the entire vibrational manifold, and D_e is the classical dissociation energy of diatomic O_2.

The conservation of vibrational energy in the STS model is formulated for each vibrational energy level. This approach significantly increases the number of equations to be solved, however it is explicitly modeling the vibrational energy behavior. Additionally, the conservation equations for species densities, given in Eq.(11) can be omitted. The system of equations for the STS model in this case accounts for the conservation of momenta and trans-rotational energy as well as for number density of individual vibrational states. The latter has the following appearance:

$$\frac{\partial n_v}{\partial x} = \sum_s \left(R_{v,s}n_O^2 n_s - D_{v,s}n_v n_s\right) + \sum_s \left(K_{v',v}n_v' n_s - K_{v,v'}n_v n_s\right),\ v = 0...v_{max} \tag{13}$$

where summation takes place over projectile species, in the present case, O_2 and O. The rates are provided in a curve fit form as shown in equation 14 and 15 for bound-bound and bound-free transition rate coefficients.

$$K_{v,v'} = 10^{-12} \times \exp\left[A_{v,v'} + B_{v,v'}/log(T/1000) + C_{v,v'}log(T/1000)\right],\ \left[cm^3/s\right], \tag{14}$$

$$D_v = A_v T^{B_v} exp\left(-C_v/T\right),\ \left[cm^3/s\right] \tag{15}$$

2. CFD Flow Solver

The computational fluid dynamics (CFD) flow simulations in this study are performed using the CFD code LeMANS.[12, 13] LeMANS is a parallel, three-dimensional code that solves the Navier-Stokes equations including thermochemical nonequilibrium effects on unstructured computational grids. LeMANS assumes that the flow can be approximated as a continuum. The standard version of LeMANS utilizes the two-temperature approach for nonequilibrium. In this approach, there is a translational temperature, T_t, and a different vibrational temperature, T_v. The other energy modes are assumed to be in equilibrium with

either the translational or vibrational temperature. For example, the rotational mode is assumed to be in equilibrium with the translational mode (i.e. $T_r = T_t$). The full details of LeMANS can be found in Ref.[12]

LeMANS has been modified to also include STS modeling of the vibrational energy mode. A master equation system is solved along with the flow equations. The inclusion of the STS modeling increases the computational time of the analysis substantially. Inherently, there are more equations to solve (47 vibrational states). Also, the system of STS equations is very stiff and requires a conservative choice in time step. Others in the industry have worked to improve the computational efficiency of the STS CFD method through various methods.[8,9] More work in this area is needed to reduce the computational expense of this type of simulation. The presented work utilized a 2T model converged solution as the initial condition for the STS analysis (assumed Boltzmann distributions). This significantly reduced the computational time, but the solution time was still around 15 times that of the nominal 2T calculation.

III.   Experimental Data

A.   Ibraguimova Shock Tube Cases

The post normal shock flow calculations are carried out for an existing set of shock tube experiments conducted by Ibraguimova et al.[30] The flow conditions for the test cases are summarized in Table3. All flow conditions have a pure O_2 freestream composition. The set of test cases represents a relevant range of conditions that might be experienced by a hypersonic vehicle.

Test case	Shock velocity $[km/s]$	$P_1 [Torr]$	$T_1 [K]$	$T_2 [K]$
C1	3.07	2.0	295	5300
C2	3.95	1.0	295	8620
C3	4.44	0.8	295	10820

Table 3.   Summary of flow conditions investigated[30]

The purpose of this experimental data comparison is to evaluate how the standard 2T model and modified 2T-NENB model perform relative to the STS results and experimental data.

B.   CUBRC Double-Cone Configuration

The double cone experimental data was obtained from the CUBRC LENS-XX expansion tunnel.[6] The focus of the work presented in this paper is on Run 87. The freestream flow conditions for Run 87 are shown in Table 4 .

Test Case	Total Enthalpy $[\frac{MJ}{kg}]$	Mach Number	Velocity $[\frac{m}{s}]$	P [Pa]	T_t	T_v	C_{O_2}	C_O
Run 87	9.9	8.1	4,019	165	626	712	0.9245	0.0755

Table 4.   Summary of flow conditions for Run 87[6]

Run 87 is a double-cone configuration. Pressure and heat transfer data was acquired at many points along the model surface. No flow field measurements were taken so only the experimental surface data will be used for model comparison. A picture and diagram[6] of the double-cone configuration are shown in Figures 9 and 10, respectively.

IV.   Results

The shock tube results focus on the effectiveness of the 2T modification (2T-NENB) when compared to a full STS analysis and experimental data. The double cone case does not have flowfield data to evaluate the nonequilibrium model details, only surface properties (pressure and heat transfer) will be used for comparison.
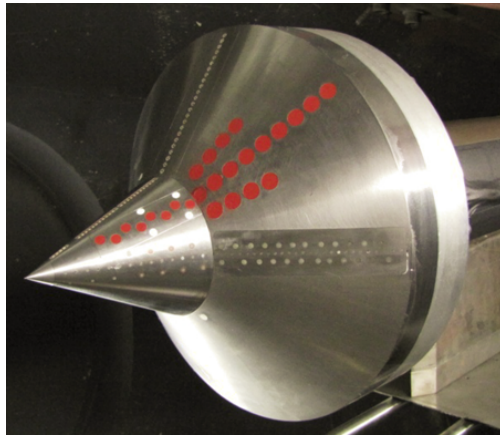
American Institute of Aeronautics and Astronautics

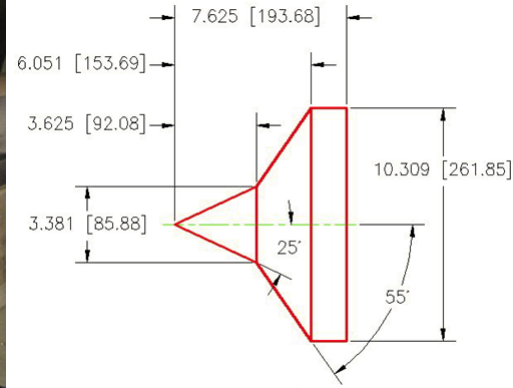Figure 9. Double-cone data points

Figure 10. Double-cone dimensions

A. Shock Tube Results
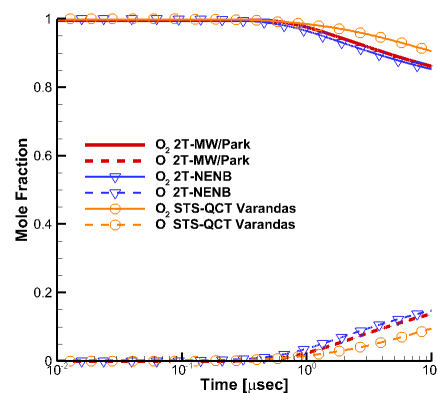
Figures 11 and 12 present the evolution of temperature and composition for the two modeling approaches for Case C1. Case C1 is a mild nonequilibrium condition in comparison to C2 and C3. The results show that the STS model produces a fundamentally different result than the 2T models. The restriction of the 2T framework for the 2T-NENB model appears to be a hindrance for replicating the STS behavior. Interestingly, the mild C1 case has the worst performance for the 2T-NENB model. It can be noted that the 2T-NENB model results suggest that it has difficulty with the VT process early (when composition is correct) and has issues with composition later in the analysis. Additionally, the population evolution is shown in Figures 21 and 22 for the STS analysis.
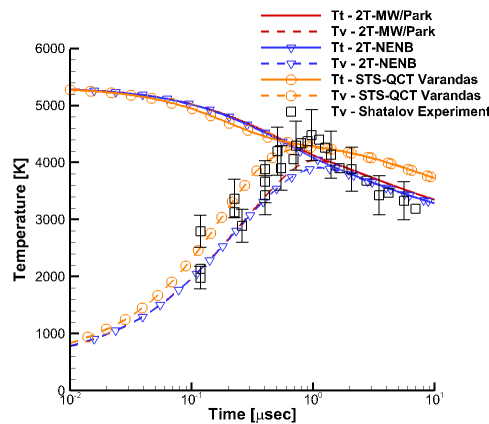
Figure 11. Temperature profiles, C1 case

Figure 12. Composition profile, C1 case

Figures 15 and 16 present the evolution of temperature and composition for the two modeling approaches for Case C2. Once again there is a fundamental difference between the STS behavior and the 2T-MW/Park model. However, the 2T-NENB does well in replicating the STS behavior. Specifically, the composition profile comparison is almost identical. This is highlighting the importance of accounting properly for the nonequilibrium and non-Boltzmann effects that are prominent in the near QSS region. There could be improvement for the VT energy transfer around the peak T_v region.

For reference, the population evolution is shown in Figures 17 and 18 for the STS analysis. These once again show the non-Boltzmann behavior in the flow.

Figures 19 and 20 present the evolution of temperature and composition for the three modeling approaches for Case C3. The difference in the behavior between the STS and 2T-MW/Park is significant once again. However, the 2T-NENB is able to capture most of the behavior observed in the STS analysis. It is not as
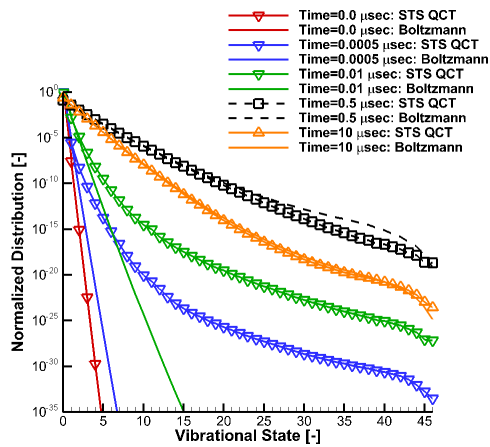
American Institute of Aeronautics and Astronautics

Figure 13. Vibrational population distribution evolution, C1 case
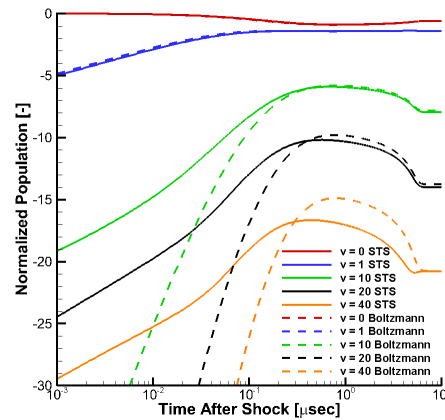

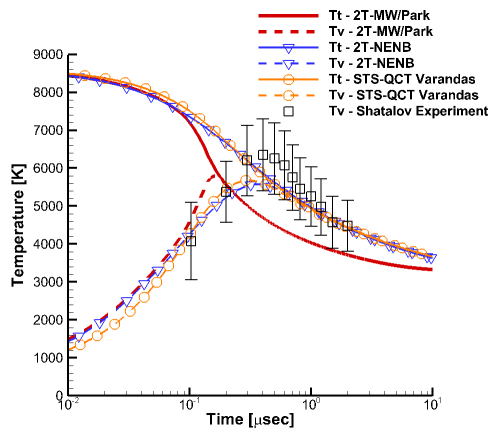**Figure 14. Vibrational state population evolution, C1 case**

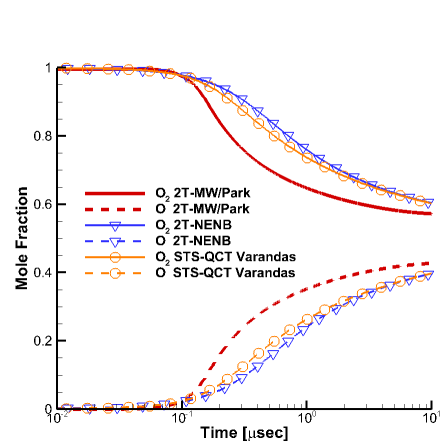**Figure 15. Temperature profiles, C2 case**

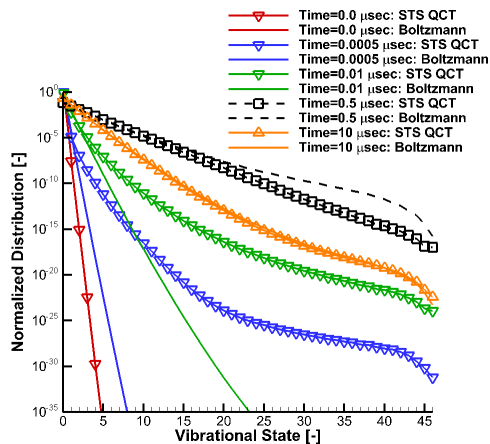**Figure 16. Composition profile, C2 case**

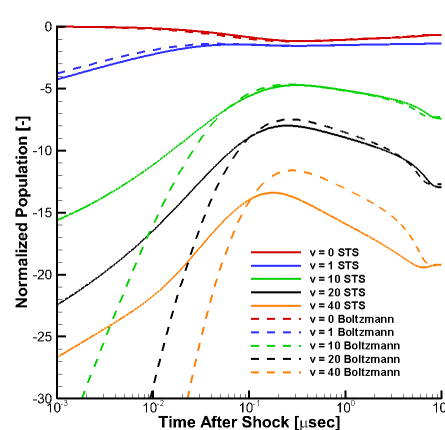**Figure 17. Vibrational population distribution evolution, C2 case**

Figure 18. Vibrational state population evolution, C2 case

precise as C2, but does retain the major features. Figures 21 and 22 present the vibrational population distribution. The behavior is similar to that described for Cases C1 and C2.
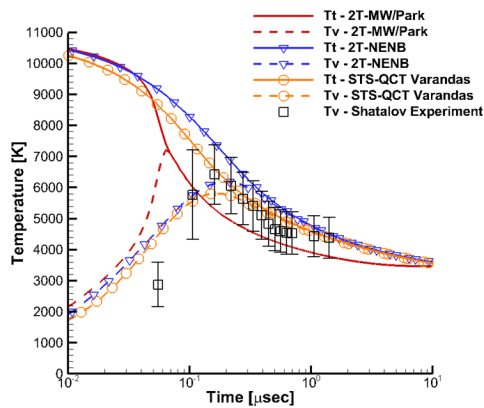
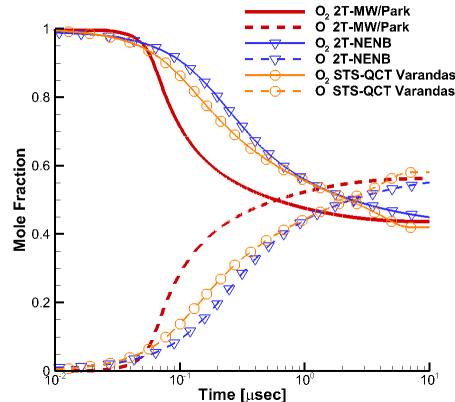**Figure 19. Temperature profiles, C3 case**

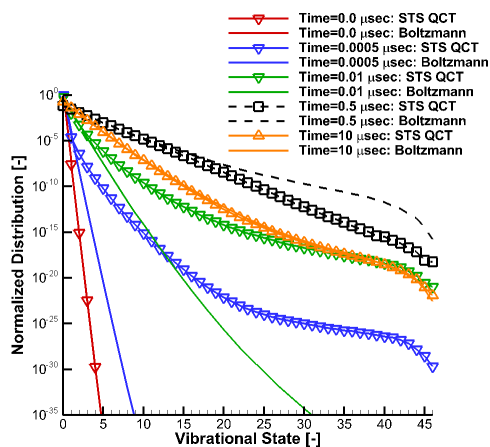**Figure 20. Composition profile, C3 case**

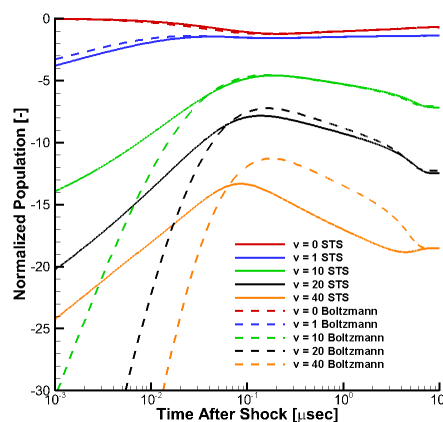**Figure 21. Vibrational population distribution evolution, C3 case**

Figure 22. Vibrational state population evolution, C3 case

The shock tube flow comparisons show a distinct and fundamental difference between the STS and 2T-MW/Park modeling results. The 2T-NENB model shows promise as a computationally inexpensive alternative to the high fidelity, STS model.

B. Double Cone Results

The CFD results shown are from an axisymmetric grid consisting of 250,000 cells. Additionally, the experiments were designed to have laminar flow so the CFD model assumes that the flow is laminar. Figure 23 presents the pressure contours for the nominal flow field of Run 87 using the standard 2T model. The flow field contains complex flow features near the double-cone transition. There is shock and boundary layer interaction along with flow separation.

Figure 24 shows the translational temperature contours for the 2T-MW/Park model. Figure 25 shows the vibrational temperature contours. The translational and vibrational temperature plots demonstrate the nonequilibrium behavior that is present in the flow field, particularly, in the second (upper) oblique shock region. The translational temperature rises quickly across the shock wave and then vibrational-translational energy transfer acts to bring the two energy modes into equilibrium downstream of the shock.

The contour plots are not able to show the differences between the different models and no experimental data was collected in the flow field. The model comparisons will be on made on the double cone surface quantities. Figures 26 and 26 present the pressure and heat transfer distributions for the three modeling types and the experimental data. The differences in the models are almost indistinguishable for surface
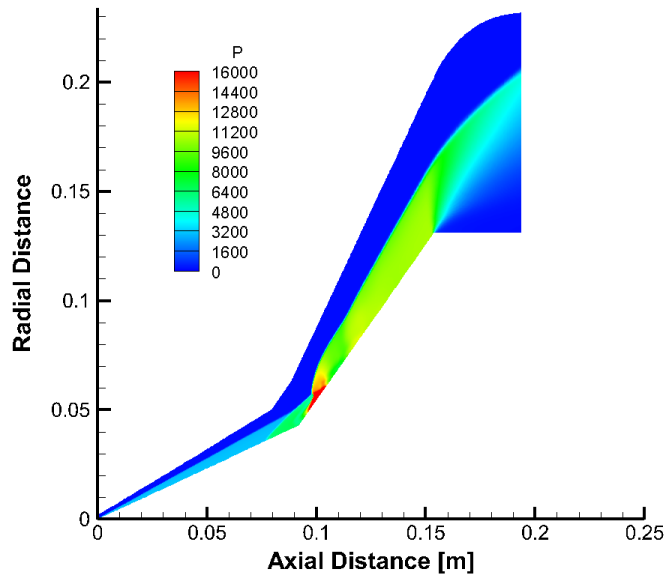
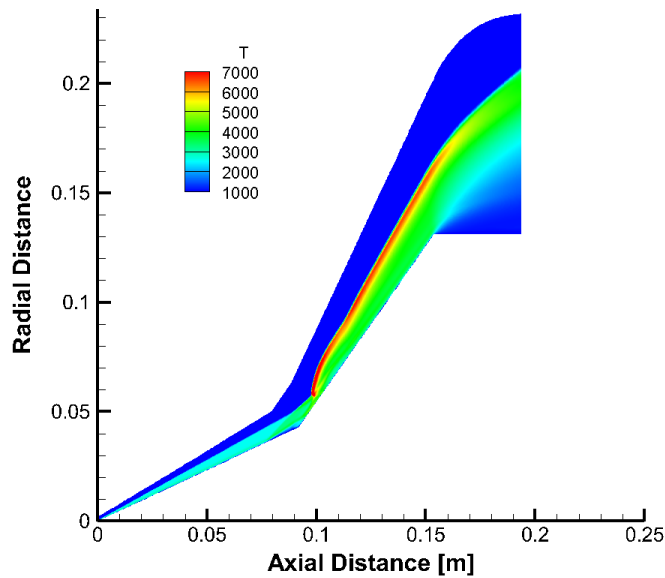**Figure 23. Pressure contour plot for nominal conditions**

Figure 24. Translational temperature contour plot for nominal conditions

quantities. All of the models possess the same features as the experimental data, however they do not capture all the features accurately. For example, the experimental data shows a sharp drop in heat transfer around an axial distance of 0.065. The models have this feature but it does not occur until an axial distance of 0.80. Given the similarity in the results presented, further work is needed to understand the differences between the CFD results and experimental data. Near wall modeling and freestream conditions are potential areas for future investigations.
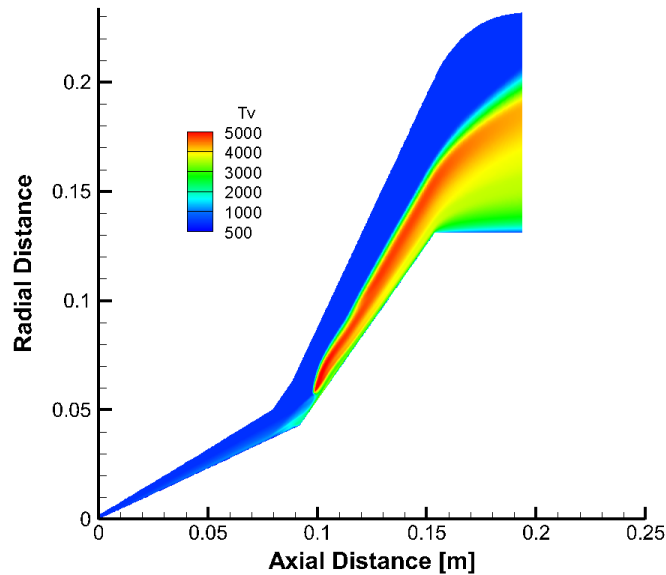
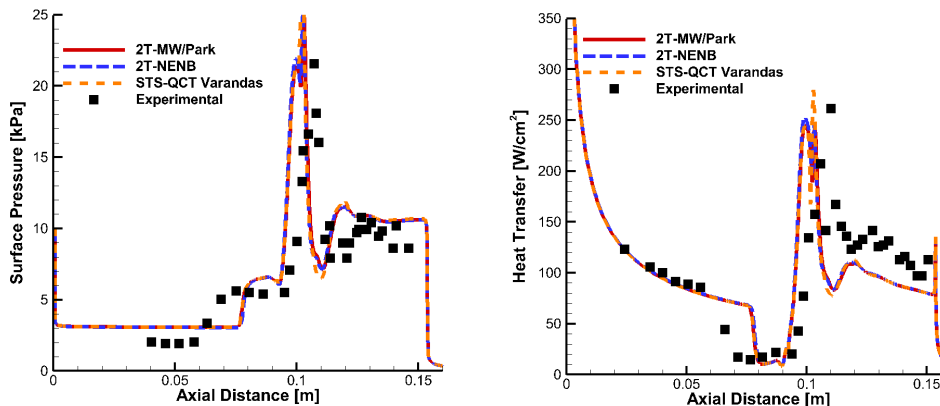**Figure 25. Vibrational Temperature contour plot for nominal conditions**

Figure 26. Pressure distribution on double cone body

Figure 27. Heat transfer distribution on double cone body

V.   Conclusions

Vibrational thermochemical nonequilibrium modeling is a critical aspect of hypersonic vehicle design. Namely, computationally efficient, reduced order models that accurately capture the relevant physics are currently required due to the current computational hardware capability and high computational cost of the high fidelity, state-to-state (STS) modeling. The two-temperature (2T) model is the state of the art thermochemical nonequilibrium model for hypersonic design work. The 2T model is powerful, but it does have its shortcomings. The 2T model is not able to capture some nonequilibrium and non-Boltzmann behavior. The presented work extends the understanding of these aspects for oxygen containing flows. Detailed STS, master equation analysis is used to evaluate the limitations of the 2T model and to suggest a modification to capture additional effects of nonequilibrium and non-Boltzmann behavior that is present in the detailed analysis. Quasi-classical trajectory (QCT) and forced harmonic oscillator (FHO) rates were

American Institute of Aeronautics and Astronautics

used for the O_2-O and O_2-O_2 systems, respectively.

The STS analysis allowed for the development of high fidelity macroscopic vibrational-translational (VT) transfer rates and total dissociation rates under nonequilibrium and non-Boltzmann conditions. This level of detail about rates is difficult, if not impossible, to capture through experimental methods. The detailed information of these nonequilibrium and non-Boltzmann effects allowed for development of the 2T-NENB model. Overall, the total dissociation rates are influenced more by these factors than the VT energy transfer. This is reflected in the model details. Specifically, the VT energy transfer adopted the QCT based function for the relaxation parameter. The 2T model already accounts properly for nonequilibrium and required only a small modification factor for non-Boltzmann effects in the 2T-NENB variant. The total dissociation rate utilizes a linear combination of translational and vibrational temperatures as a control temperature to account properly for nonequilibrium effects. Additionally, a scale parameter is introduced to account for non-Boltzmann effects.

Shock tube flow and double cone experimental data was used to evaluate the models for accuracy. The shock tube results show that the 2T-NENB model is able to improve on the deficiencies observed in the standard 2T model. The simple modification terms are able to account for nonequilibrium more precisely and account for the impact of non-Boltzmann distributions. Future work may include incorporating more complexity in order to better represent detailed physics in the thermochemical behavior. The double cone analyses show some discrepancies between the various models and the experimental surface data. This difference suggests that further investigation is needed in the near wall behavior of nonequilibrium CFD and perhaps the determination of the freestream conditions of the experiments.

Acknowledgments

References

[1] K. Edquist, A. Dyakonov, M. Wright, C. Tang, "Aerothermodynamic Design of the Mars Science Laboratory Heatshield," AIAA 2009-4075, 41st AIAA Thermophysics Conference, San Antonio, Texas, June 2009.

[2] D. Olynick, Y.K. Chen, M. Tauber, "Forebody TPS Sizing with Radiation and Ablation for the Stardust Sample Return Capsule," AIAA 97-2474, AIAA, June 1997.

[3] D. Kinney, "Development of the ORION Crew Exploration Vehicles Aerothermal Database Using A Combination of High Fidelity CFD and Engineering Level Methods," AIAA 2009-1100, 47th AIAA Aerospace Sciences Meeting, Orlando, Florida, January 2009.

[4] G. Candler, I. Nompelis, M. Druguet, M. Holden, T. Wadhams, I. Boyd, W. Wang, "CFD Validation of Hypersonic Flight: Hypersonic Double-Cone Flow Simulations," RTO-TR-AVT-007, 40th AIAA Aerospace Sciences Meeting, Reno, Nevada, January 2002.

[5] M. Holden, T. Wadhams, M. MacLean, "A Review of Experimental Studies with the Double Cone and Hollow Cylinder/Flare Configurations in the LENS Hypervelocity Tunnels and Comparisons with Navier-Stokes and DSMC Computations," AIAA 2010-1281, 48th AIAA Aerospace Sciences Meeting, Orlando, Florida, January 2010.

[6] M. Holden, T. Wadhams, M. MacLean, A. Dufrene, "Measurements of Real Gas Effects on Regions of Laminar Shock Wave/Boundary Layer Interaction in Hypervelocity Flows for Blind Code Validation Studies," AIAA 2013-2837, 21st AIAA CFD Conference, San Diego, California, June 2013.

[7] K. Neitzel, D. Andrienko, I.D. Boyd, "Modeling Fidelity for Oxygen Nonequilibrium Thermochemistry in Reflected Shock Tube Flows," 46th AIAA Thermophysics Conference, AIAA Paper 2015-2509, June 2015.

[8] P. Vedula, E. Josyula, "Numerical Simulation of Hypersonic Blunt Body and Nozzle Flows using Master Equation," 10th AIAA/ASME Joint Thermophysics and Heat Transfer Conference, AIAA Paper 2010-4331, July 2010.

[9] J. Burt, E. Josyula, "Assessment of Vibrational Nonequilibrium for State Resolved Simulation of a Hypersonic Flow," 54th AIAA Aerospace Sciences Meeting, AIAA Paper 2016-0737, January 2016.

[10] A. Brandt, "Guide to Multigrid Development," Springer-Verlag, 1982.

[11] A. Brandt, "Barriers to achieving textbook multigrid efficiency (TME) in CFD," ICASE Interim Report No. 32 NASA/CR-1998-207647, 1998.

[12] L. Scalabrin, "Numerical Simulation of Weakly Ionized Hypersonic Flow over Reentry Capsules," Ph.D. thesis, University of Michigan, 2007.

[13] A. Martin, L. Scalabrin, I.D. Boyd, "High Performance Modeling of Atmospheric Re-entry Vehicles," Journal of Physics: Conference Series, Vol. 341, No. 1, 2012, Article 012002.

[14] C. Park, "Nonequilibrium Hypersonic Aerothermodynamics," *Wiley*, New York, 1990, pp. 119-144.

[15] R.C. Millikan and D.R. White, "Systematics of vibrational relaxation," *The Journal of Chemical Physics*, Vol. 39, No. 12, p. 3209, 1963.

[16]F. Thivet, M.Y. Perrin, S. Candel, "A unified nonequilibrium model for hypersonics," *Physics of Fluids*, Vol. 3, p. 2799, 1991.

[17]C. Park, "Review of Chemical-Kinetic Problems of Future NASA Missions, I: Earth Entries," *Journal of Thermophysics and Heat Transfer*. Vol. 7, No. 3, 1993, pp. 385-398.

[18]D. Andrienko, I.D. Boyd, "Vibrational Relaxation and Dissociation of Oxygen in Molecule-Atom Collisions," 46th AIAA Thermophysics Conference, AIAA Paper 2015-3251, June 2015.

[19]K. Neitzel, J.G. Kim, I.D. Boyd, "Nonequilibrium Modeling of Oxygen in Reflected Shock Tube Flows," 45th AIAA Thermophysics Conference, AIAA Paper 2014-2961, June 2014.

[20]J.G. Kim and I.D. Boyd, "State-resolved master equation analysis of thermochemical nonequilibrium of nitrogen," *Chemical Physics*, Vol. 415, p. 237-246, 2013.

[21]I.V. Adamovich and J.W. Rich, Threedimensional nonperturbative analytical model of vibrational energy transfer in atom-molecule collisions, *Journal of Chemical Physics*, Vol. 109, No. 18, 1998, pp. 7711-7724.

[22]I.V. Adamovich, S.O. Macheret, J.W. Rich, and C.E. Treanor, Vibrational Relaxation and Dissociation Behind Shock Waves Part 2: Master Equation Modeling, *Journal of Thermophysics and Heat Transfer*, Vol. 33, No. 6, 1995, pp. 1070-1075.

[23]I.V. Adamovich, Three-dimensional Analytic Model of Vibrational Energy Transfer in Molecule-Molecule Collisions, *AIAA Journal*, Vol. 39, No. 10, 2001, pp. 1916-1925.

[24]F. Esposito, I. Armenise, G. Capitta, M. Capitelli, "O-O_2 state to state vibrational relaxation and dissociation rates based on quasiclassical calculations," *Chemical Physics*. Vol. 351, 2008, pp. 91-98.

[25]M. Lino da Silva, J. Loureiro, V. Guerra, A multiquantum dataset for vibrational excitation and dissociation in high-temperature O_2-O_2 collisions, *Chemical Physics Letters*, Vol. 531, 2012, pp. 28-33.

[26]F. Esposito and M. Capitelli, "The relaxation of vibrationally excited O_2 molecules by atomic oxygen," *Chemical Physics Letters*, Vol. 443, p. 222-226, 2007.

[27]F. Esposito, I. Armenise, G. Capitta, and M. Capitelli, "O+O_2 state-to-state vibrational relaxation and dissociation rates based on quasiclassical calculations," *Chemical Physics*, Vol. 351, pp. 91-98, July 2008.

[28]J. Breen, R. Quy, G. Glass, "Vibrational relaxation of O_2 in the presence of atomic oxygen," *The Journal of Chemical Physics*, Vol. 59, p. 556-557, 1973.

[29]K. Fujita, "Influences of Molecular Rotation on Vibrational Kinetics and Dissociation of N2," 48th AIAA Aerospace Sciences Meeting, AIAA Paper 2010-1568, January 2010.

[30]L.B. Ibraguimova, A.L. Sergievskaya, V.Yu. Levashov, O.P. Shatalov, Yu.V. Tunik, "Investigation of oxygen dissociation and vibrational relaxation at temperatures 4,000-10,800K," *The Journal of Chemical Physics*, Vol. 139, p. 034317-034328, 2013.

[31]B. Lopez, M. Lino da Silva, "Non-Boltzmann Analysis of Hypersonic Air Re-Entry Flows," AIAA Paper 2014-1889955, June 2014.

[32]R. Jongma, A. Wodtke, "Fast multiquantum vibrational relaxation of highly vibrationally excited O_2," *The Journal of Chemical Physics*, Vol. 111, p. 10957-10963, 1999.

American Institute of Aeronautics and Astronautics